Design of selective chemical probes for the serum and glucocorticoid-regulated kinase SGK3

Julian Blagg[a], Jon Roffey[a], Caryn Ross-Innes[a], Arwel Lewis[b], Michael Goldsmith[b], Chris Brown[b], Isabelle Lemasson[b], Ben Sutton[b], Silvia Bonomo[b], Alicia Higueruelo[b], Chigozie Achara[b], Alex Groarke[b], Shilina Roman[b], Susanna Stimpson[b], Stefano Pernigo[b] and Nicole Hamblin[b]

[a] Azeria Therapeutics, Cambridge, UK. [b] Charles River, Chesterford Research Park, Saffron Walden, UK.

1 Introduction

The serum and glucocorticoid kinases (SGKs), a subfamily of the AGC kinases, are comprised of three highly homologous isoforms. SGKs are regulated by growth factors, cytokines and cell stressors and regulate ion channel activity through serine and/or threonine phosphorylation.

SGKs have been increasingly implicated in oncogenic signaling, most notably in estrogen receptor positive (ER+) breast cancer including endocrine therapy resistant disease of significant medical need.[1] SGK1 and SGK3 become essential in models of ER+ve breast cancer where AKT or PI3K is inhibited; consequently, additional antiproliferative effects are achieved with combinations of an SGK degrader and a PI3K or AKT inhibitor in models of ER+ve breast cancer compared to treatment with PI3K or AKT inhibitors alone.[2]

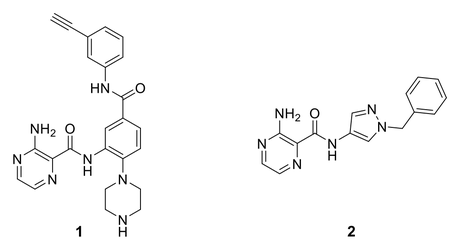

Fig.1 Novartis pan-SGK inhibitor **1** and HTS hit **2** (SGK3 IC_{50} = 3.2 μM)

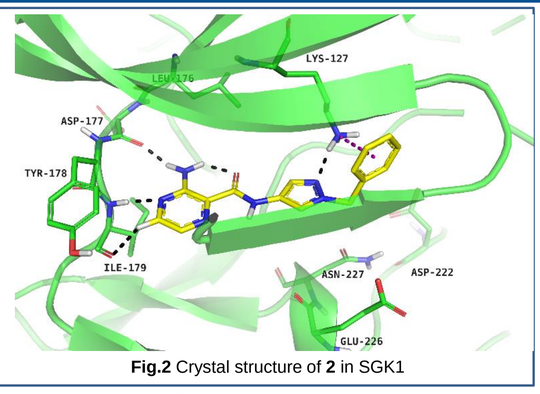

Fig.2 Crystal structure of **2** in SGK1

SGK-family inhibitors reported to date include azaindoles from GSK,[3] pyrazolopyrazines from Sanofi,[4] and aminopyrazines from Novartis.[5] We sought to develop potent, SGK3-selective inhibitors to further investigate the role of this isoform in ER+ve breast cancer. High-throughput screening of a 167K Charles River compound library using a TR-FRET biochemical assay *vs* SGK3 led to identification of the pyrazole amide hit **2**, which shares the same hinge-binding motif as the Novartis pan-SGK inhibitor **1** (**Fig.1**).

A co-crystal structure of hit compound **2** with SGK1 (**Fig.2**) revealed three hydrogen bonding interactions between the amino pyrazine and SGK3 hinge residues Asp177 and Ile179. The unsubstituted pyrazole nitrogen is positioned to H-bond with Lys127 and this residue lies in an optimal orientation to form a π-cation interaction with the phenyl ring of the pyrazole benzyl substituent.

Key objectives:

- Use structure-based design to discover analogues of **2** with increased SGK3 potency and selectivity over off-targets from the AGC family such as AKT2 and ROCK1.
- Improve the DMPK profile *vs* the poorly water soluble and amidase-susceptible Novartis aminopyrazine **1** to enable evaluation of *in vivo* effects on biomarkers of SGK3 activity.

2 Improving SGK3 potency

- SGK3 activity was improved *via* the enhanced π-cation interaction achieved with the more electron-rich 3-methoxybenzyl substituent of **3**. Taking inspiration from similar approaches in the literature,[6] addition of a basic substituent at the benzylic position also improved activity (**4**); a co-crystal structure of **4** in SGK1 demonstrated additional interactions between the basic centre and an acidic patch around Glu226 (**Fig.3**).
- The beneficial effects of the basic group and electron-rich aromatic were combined in **5**, displaying ~50-fold greater potency than the hit **2**. The eutomer was determined to be the *S*-enantiomer by small molecule X-ray crystallography; its enantiomer was ~25-fold less potent.
- Modifications to the pyrazole ring (alternative heterocycles or incorporation of substitution) or linking amide were poorly tolerated, and only *meta*-substituted benzyl groups generally conferred good SGK3 potency.

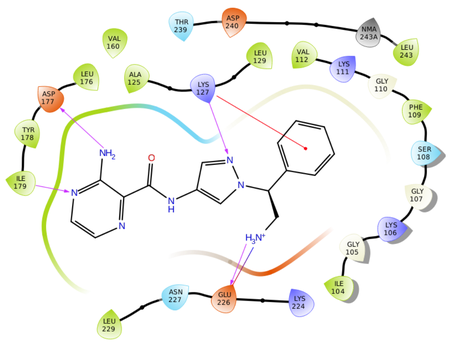

Fig.3 2D representation of co-crystal structure of **4** in SGK1

	Compound	1 (Novartis)	2	3	4	5	6
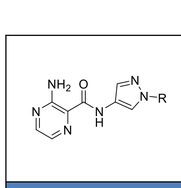	R =	-	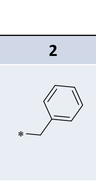	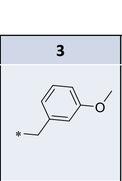	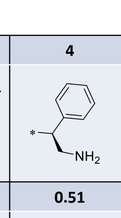	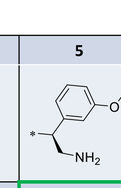	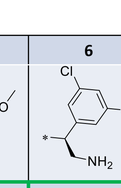
Potency & Selectivity	SGK3 IC_{50} (μM)	0.016	3.2	0.84	0.51	0.069	0.073
	SGK1 IC_{50} (μM)	0.019	-	4.3	3.07	2.2	8.4
	AKT2 IC_{50} (μM)	-	>10	>10	-	-	-
	ROCK1 IC_{50} (μM) (selectivity for SGK3 over ROCK1)	>30 (x>1000)	0.49 (×0.15)	0.095 (×0.1)	0.51 (×1)	0.027 (x0.4)	0.29 (x4)
	MCF7-pSer330-NDRG1 (IC50) (μM)	2.9	-	>10	0.08	0.13	6.1
in vitro ADME	MLM/HLM Clint (μL/min/mg)	32 / <15	75 / 96	47 / 70	<14 / <14	<14 / 35	29 / 75
	Caco-2 A>B / efflux	2.9 / 55	-	51 / 1.1	42 / 1.0	18 / 1.4	19 / 1.7
	Mouse AO $t_{1/2}$ (h)	1.9	>10	>10	3.8	>10	-
in vivo PK (mouse) *i.v.* 1 mg/kg *p.o.* 5 mg/kg	Cl (mL/min/kg)	487	-	31	53	23	-
	$t_{1/2}$ (hr)	0.85	-	0.35	1.7	2.2	-
	V_{ss} (L/kg)	25	-	0.52	7.5	3.6	-
	F %	-	-	-	42	79	-

4 Building selectivity over ROCK1

- Generation of enhanced selectivity against other members of the AGC kinome such as the AKTs and ROCK1 was a key objective to deconvolute observed biological effects and to mitigate against associated downstream risk. While representative compounds derived from **2** did not bind to AKT2, significant ROCK1 inhibition was observed. The acetylene-substituted phenyl ring of Novartis compound **1** occupies a deep pocket beyond the gatekeeper in the SGKs that is occluded by bulky Met residues in ROCK1; a vector to occupy this pocket was unavailable in the pyrazole series, necessitating investigation of alternative mechanisms for generation of selectivity over ROCK1.
- SAR development around the terminal aryl ring showed that incorporation of a *meta* chloro substituent imparted modest selectivity for SGK3 over ROCK1 (compound **6**), an observation not readily explained by examination of the protein structures in this region. Subsequent optimisation of the hinge binding amino-heterocycle of **6** showed that a substituted pyrazine or pyrimidine afforded a further improvement in selectivity, *i.e.* **7 - 9**.

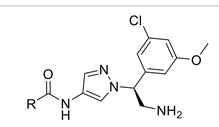

	7	8	9	*d*-9	10
	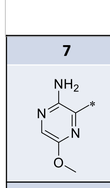	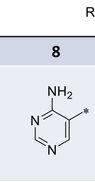	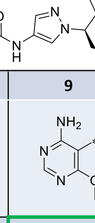	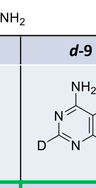	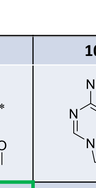
	0.11	0.75	0.069	0.065	0.27
	1.7	6.4	1.9	2.0	1.5
	-	-	>10	-	>10
	1.58 (×14)	8.9 (×12)	1.03 (×15)	1.7 (×26)	18 (×59)
	-	-	-	-	-
	25 / 73	19 / <28	20 / 111	25 / 108	54 / 54
	22 / 1.7	<0.36 / >71	20 / 4.0	19 / 4.9	-
	-	3	1.9	7.8	-
	28	59	-	22	-
	1.3	1.5	-	3.3	-
	2.4	5.1	-	4.0	-
	29	-	-	36	-

- Docking studies suggested that bulkier bicyclic hinge binding motifs such as the imidazopyrimidine of **10** could be accommodated in the SGKs (**Fig.6**) but not ROCK1, where a bulkier Phe residue occupies the position of Leu229. This theory was validated by screening data, with **10** showing significantly improved selectivity for SGK3.

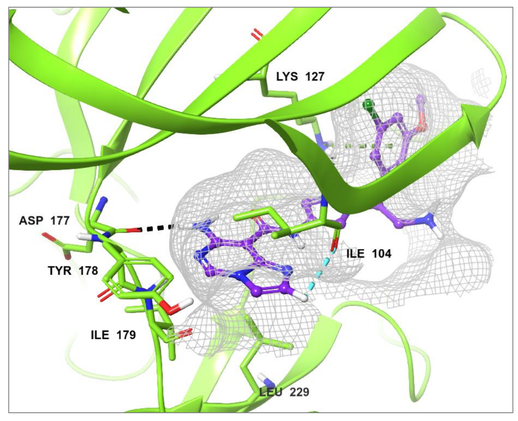

Fig.6 Docking of **10** in SGK1 crystal structure

3 DMPK profiling and *in vivo* biomarker modulation

- Incorporation of the basic substituent in **4** afforded increased *in vitro* microsomal stability compared to neutral analogues **2** & **3**. Compounds across the series had high aqueous solubility (*e.g.* 185 μM for **4**), in contrast to the Novartis inhibitor **1** (<5 μM).
- Despite the presence of 5 hydrogen bond donors, **4** was permeable in Caco-2 cells without significant efflux, which we attributed to masked polarity *via* an extensive network of intramolecular H-bonds.
- Cellular activity was evaluated by measurement of inhibition of phosphorylation of the SGK3 substrate *N*-Myc Downstream Regulated 1 (NDRG1) in the MCF7 cell line, with the aminomethyl analogues **4** & **5** displaying sub-micromolar potency.
- Potent analogue **5** showed moderate clearance and good oral bioavailability in a mouse PK study and was progressed to *in vivo* biomarker evaluation, measuring pS330-NDRG1 levels in an MCF7 human tumour xenograft model in female athymic nude mice.
- >50% target receptor occupancy was achieved up to 12 h in both plasma and tumour (**Fig.4**), which resulted in significant reduction of pS330-NDRG1 levels compared to vehicle up to 24 h post-dose (**Fig.5**).

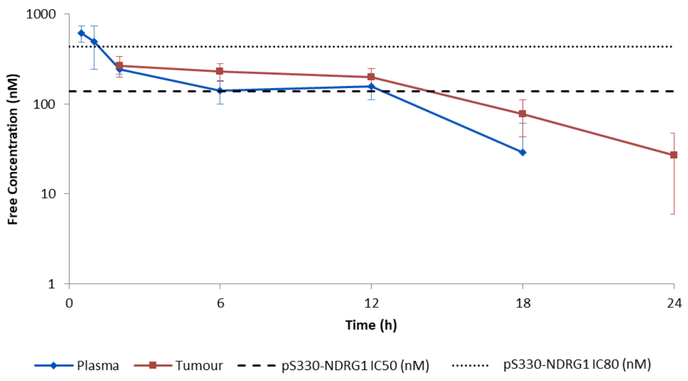

Fig.4 Receptor occupancy following a single oral dose of **5** @ 15 mg/kg

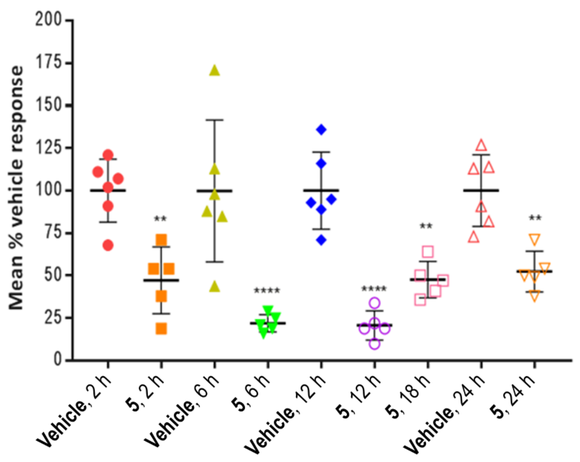

Fig.5 pSer330-NDRG1 levels following single oral dose of **5** @ 15 mg/kg

5 Towards an improved ADME profile

- Although pyrimidine **8** improved selectivity over ROCK1 compared to the corresponding pyrazine **6**, activity at SGK3 was reduced 10-fold and the compound suffered from very low Caco-2 permeability with high efflux. We suspected these issues to be the result of loss of an intramolecular H-bond between the pyrazine nitrogen atom and the linking amide, causing an unfavourable conformational change and exposure of polarity. Reintroduction of the H-bonding interaction by installation of a methoxy substituent in **9** led to recovery of the lost potency, significantly improved permeability and mitigation of efflux.
- Pyrimidines **8** and **9** were shown to be susceptible to metabolism by aldehyde oxidase. Deuteration at the 2-position of **9** significantly increased half-life *in vitro* (kinetic deuterium isotope effect = 4.1) and translated to relatively low clearance *in vivo* for *d*-**9**.

6 Conclusions

- Structure-based optimisation of a 3 μM SGK3 pyrazole amide screening hit led to the identification of a sub-set of basic analogues with ~50-fold improved potency and attractive PK properties that demonstrated *in vivo* modulation of the SGK3-relevant biomarker pNDRG1.
- Selectivity issues with the AGC-family kinase ROCK1 were addressed by modification of the pendent aromatic ring and hinge binding heterocycle.
- Despite clear evidence for target engagement, these optimized chemical probes failed to demonstrate significant anti-proliferative activity in ER+ve cell lines including cells representative of therapy-resistant contexts casting doubt upon the therapeutic potential of SGK3 inhibition as a monotherapy in ER+ve breast cancer.

7 References

1. Alessi *et al, EMBO J.*, 2016, 35, 1902.
2. Ciulli *et al, ACS Chem. Biol.*, 2019, 14, 2024.
3. Hammond *et al.*, *Bioorg. Med. Chem. Lett.*, 2009, 19, 4441.
4. Halland *et al., ACS Med. Chem. Lett.* 2015, 6, 73.
5. ACS Abstract, 253rd ACS, April 2017.
6. Zhan *et al., European Journal of Medicinal Chemistry,* 2016, 117, 47.